Journal of Applied Electrochemistry **29**: 1177–1183, 1999.

Effect of nonaqueous anodic oxidation on the intensity of photoluminescence of porous silicon

M. SHIMURA*, M. KATSUMA, T. CHIKUMA and T. OKUMURA
Department of Electronics & Information Engineering, Tokyo Metropolitan University, Hachioji, Tokyo 192-0397, Japan
*(*author for correspondence)*

Received 17 March 1998; accepted in revised form 16 February 1999

Key words: anodic oxidation, ethylene glycol, peeling, photoluminescence, porous silicon

Abstract

Porous silicon (PS) was anodized for short periods in 0.02 M KNO_3–ethylene glycol electrolyte to improve the maximum intensity of its photoluminescence (PL) by changing surface –Si–H bonds to –Si–OH or –Si–O-related compounds. A PS sample prepared in 1:1 (49% HF:99.5% EtOH) electrolyte gave 15-fold PL intensity as well as stabilized luminescence with 5 min anodization. Prolonged anodization, however, peeled off the nano-ordered silicon particles and resulted in a decrease in PL intensity. The PL intensity of the PS sample prepared in 1:2 electrolyte decreased with 1 min anodization but increased with 30 s anodization. During anodization, the nano-ordered silicon particles reacted with water, an impurity in ethylene glycol, to give Si–OH and Si–O-related compounds. Ethylene glycol proved to be the best anodization solvent for nano-ordered silicon particles because of its high resistivity, high viscosity, and good electrochemical stability. However, ethylene glycol had to be removed completely from the PS surface by rinsing with pure water, because polyhydroxy alcohols such as ethylene glycol behaved as quenchers for excited electrons formed in Si–OH-related compounds on the nano-ordered silicon as a result of illumination.

1. Introduction

When PS is subjected to heat treatment (< 600 °C) in air (O_2) or light illumination, the maximum intensity (I_{max}) of its visible photoluminescence (PL) decreases [1, 2] and the maximum wavelength (λ_{max}) is shifted to the blue wavelength region [3–5]. The decrease in intensity is brought about by nonradiative deactivation of excited excited electrons due to the formation of dangling bonds [2–10] which are produced by thermal or photoscission of terminal Si–H at the surface. The blue shift of λ_{max} is induced by a decrease in quantum size [11–14] and by the formation of –Si–O compounds on the nano-ordered surface [15, 16]. When the surface is covered with –Si–O compounds, excited electrons in the nano-ordered silicon recombine with holes through the levels in the compounds and thus the emission energy is increased [15, 16].

Batstone et al. [17] reported that whenever the nano-ordered particles are covered with stable oxide films after heating for a few minutes at 950 °C, the I_{max} of PL is stabilized. Our study is aimed at increasing and stabilizing the intensity of PL by quickly oxidizing nano-ordered silicon electrochemically [18–21]. Electrochemical reactions are superior to conventional chemical reactions in the following respects. At anodic polarization, the Gibbs free energies of oxidants as products decrease, resulting in a decrease in the activation energy of reductants as reactants [22, 23]. Thus, the reaction proceeds as it would at high temperatures. Similar to the oxidation of Al [24–29], the oxidation of –Si–H to –Si–O compounds in an aqueous system can be expressed by the elementary processes (Reactions 1–4) [30–32].

$$-(Si)_n\text{–}H \rightarrow -(Si)_n + H^+ + e^- \quad (1)$$

$$-(Si)_n + H_2O \rightarrow -(Si)_nOH_2 \quad (2)$$

$$-(Si)_nOH_2 \rightarrow -(Si)_nOH + H^+ + e^- \quad (3)$$

$$-(Si)_n\text{–}OH \rightarrow -(Si)_n\text{–}O + H^+ + e^- \quad (4)$$

On the other hand, the overall equilibrium potential of a reaction between Si and H_2O, that is,

$$Si + 2\,H_2O = SiO_2 + 4\,H^+ + 4\,e^-,$$

is given by $E_0 = -0.857 - 0.059$ pH [23]. The equilibrium potential shifts to more negative values with

decreasing H^+ concentration. This implies that Si can be more easily oxidized in an aqueous system in accordance with the decrease in H^+ concentration and a more negative voltage is necessary to suppress Si oxidation. The applied voltages contribute to the lowering of the activation energies of Reactions 1, 3 and 4 in addition to the lowering of the space charge barrier of the porous silicon surface. H^+ generated in Reaction 1, 3, and 4 moves to the bulk of the electrolyte. In an acidic electrolyte, however, H^+ concentration is higher in the bulk of the electrolyte than in the vicinity of the anode, and the concentration gradient is opposite to the direction of the migration. Accordingly, H^+ is pushed back to the anode and the removal of H^+ from the anode becomes difficult. For Reactions 1 to 4 to proceed easily, it is necessary to use electrolytes with low H^+ concentration (e.g., non-aqueous solvents). Ethylene glycol (although containing 5% H_2O) is a nonaqueous solvent with reasonably high viscosity and surface tension, high resistivity and good electrochemical stability. Solvents with low viscosity and low surface tension easily penetrate into the interstices of nano-ordered silicon. In the case of low electrical resistivity, anodic oxidation starts at the bottom of the porous layer whenever the solvent penetrates into the bottom, and thus the top surface is not subjected to the anodic oxidation. In an electrochemically unstable (easily oxidizable) solvent, oxidation of the solvent is predominant and the oxidation of silicon does not proceed as long as the solvent exists.

2. Experimental details

PS samples were prepared from p-type silicon wafers (1 0 0) of about 14 Ω cm with anodic etching in 1:1, 1:2, 1:4 mixed electrolytes of HF (49%)–EtOH (99.5%) at 20 mA cm^{-2} for 30 min. The PS samples were then anodized at 20 mA cm^{-2} in 0.02 M KNO_3–ethylene glycol electrolyte for between 15 s–30 min at 25 °C. For comparison, the PS samples were anodized in 0.02 M KNO_3–H_2O or HCl–H_2O (1:7) electrolyte for 10 min. Furthermore, p-type silicon wafers (1 0 0) were anodized in 0.02 M KNO_3–EG electrolyte for 10 min. The anodized samples were rinsed thoroughly with pure water and dried in nitrogen gas.

The PL was measured with the excitation 420 nm light from a 150 W xenon lamp using a Hitachi F-4500 fluorescence spectrophotometer after exposing the sample to air for at least 20 min.

The sizes of nano-ordered silicon particles were estimated from their Raman spectra using a Raman laser spectrometer (spectrometer: Jeol JRS–400D) and an argon laser (NEC GCS–3200). The composition of the PS sample was measured using a JASCO–5300 Fourier transform infrared spectrophotometer. The surfaces and cross sections of PS samples were observed using high-resolution SEM and TEM.

3. Results and discussion

3.1. *Change in PL with anodization*

As shown in Figure 1(a), I_{max} of the PL, which was emitted from a PS sample prepared in 1:1 (49% HF:99.5% EtOH) electrolyte, increased 15-fold (0 min: 90 [arb. unit] → 5 min: 1350 [arb. unit]) with the anodic oxidation in 0.02 M KNO_3–EG electrolyte at 20 mA cm^{-2} for 5 min. At the same time, the maximum wavelength (λ_{max}) shifted to the shorter wavelength region; 0 min: > 800 nm (< 1.55 eV), → 5 min: approx. 750 nm (1.65 eV) → 10 min: 650 nm (1.91 eV). These changes are explained by the surface oxidation [11, 12] of nano-ordered silicon particles, which brings about a decrease of the particles size [11–14], and the formation of fluorphors such as –Si(OH)H compounds [33]. However, the prolonged anodization for over 10 min led to a drop of I_{max} for a PS sample prepared in the 1:1 electrolyte. This was caused by peeling off of the dense surface layer consisting of nano-ordered silicon particles, as clarified from high resolution TEM images. The reason for this was analysed as follows. The anodic current could not flow continuously on the top surface of nano-ordered particles [21] because of the formation

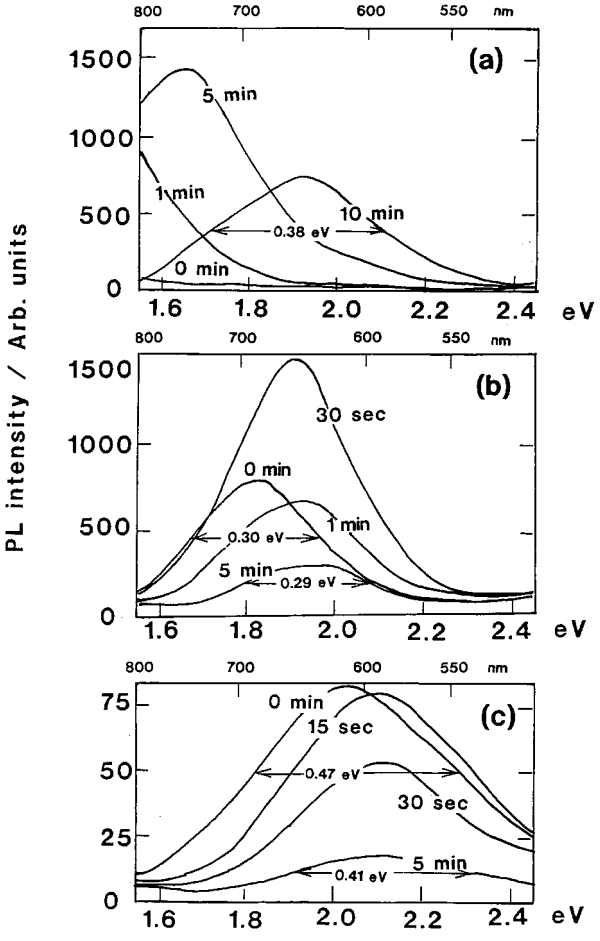

Fig. 1. Changes in PL of porous silicon prepared at 20 mA cm^{-2} for 30 min in (a) 1:1, (b) 1:2, (c) 1:4 (49% HF:99.5% EtOH) electrolytes, with anodization in 0.02 M KNO_3–EG electrolyte.

of a resistive Si–O film. Accordingly, it concentrated in the underlying particles which were not yet oxidized. With the passage of a concentrated current (i.e., high current density), the underlying particles [21] were immediately oxidized. The oxidation breaks the >Si–Si< bond of the nano-ordered particles into two >Si–O bonds and changes into more fragile species, so that the dense surface layer peels off.

For a PS sample prepared in 1:2 electrolyte, anodization for 1 min led to a decrease in I_{max} of PL (Figure 1(b)). By shortening the anodization time to 30 s, however, a considerable increase in I_{max} (710 → 1340 [arb. units]) was observed. This can be explained by the fact that the oxidized nano-ordered silicon particles which produce PL emission [33] remain on the surface of the PS sample. Since the sizes of the nano-ordered silicon particles were estimated from its Raman shift and width [34] to be smaller than (< 3.9 nm) those of particles prepared in the 1:1 electrolyte (> 5 nm), the electric charge required for surface oxidation is less and thus excess oxidation splits $–(Si–Si)_n$ bonds of the particles into $–(Si)_{n/2}–O$ and $O–(Si)_{n/2}–$, resulting in peeling. For the PS sample prepared in the 1:4 electrolyte, anodization for 15 s led to a decrease in I_{max} of the PL, while λ_{max} slightly shifted to the blue wavelength region (Figure 1(c)). This shows that anodization started on the nonnano-ordered surface at the bottom of the PS layer, since a large part of the dense layer peeled off during preparation in the 1:4 electrolyte (see Figure 6(a)).

Apart from the above behavior, we found that I_{max} decreased with the adsorption of alcoholic OH groups which acted as quenchers for the excited electrons in the nano-ordered silicon particles, especially for the as-prepared PS samples, the details of which have been discussed elsewhere [35, 36].

3.2. *Time profile of cell voltage at the anodization of PS samples*

Figure 2 shows time profiles of cell voltages for anodization in 0.02 M KNO_3-EG electrolyte for PS samples prepared in 1:1 (a), 1:2 (b), and 1:4 (c) electrolytes. The inset is an enlargement of the initial stage of (c). At the initial stage (a: 0 ~ 4 min, b: 0 ~ 30 sec and c: 0 ~ 3 sec), the cell voltages decrease slightly in spite of the formation of resistive Si–O. This suggests that the nano-ordered surfaces contacting the EG electrolyte extend gradually with the diffusion of the electrolyte and thus the "real" current densities decreases. During the next stage, where the cell voltage increases, it is considered that the nano-ordered surface is entirely coated with resistive Si–O and the charge transferring surfaces decrease due to the peeling off of most of the nano-ordered particles to result in an increase in "real" current density. When the anodization was carried out in aqueous 0.02 M KNO_3 electrolyte, however, cell the voltages increase abruptly after a short initial stage of 0 ~ 30 and 0 ~ 10 sec for PS samples prepared in 1:1 (a)

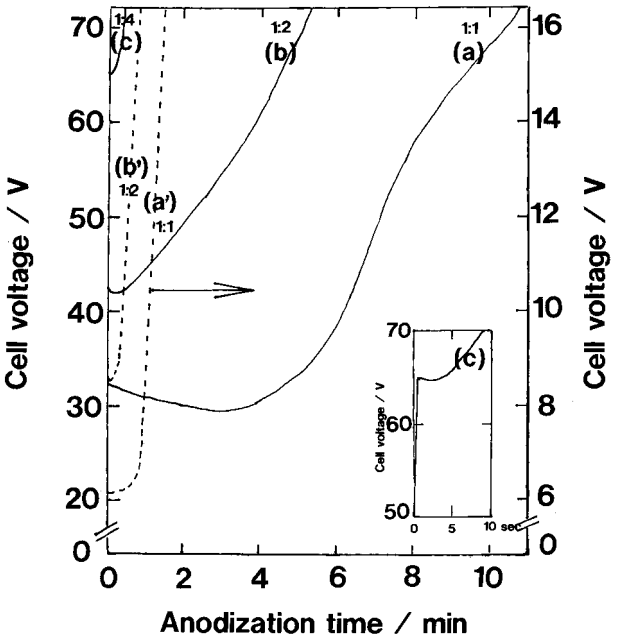

Fig. 2. Time profiles of cell voltages in 0.02 M KNO_3–EG electrolyte at anodization of PS samples prepared in 1:1 (a), 1:2 (b) and 1:4 (c) HF–EtOH electrolytes. (a′) and (b′): in aqueous 0.02 M KNO_3 electrolyte. Inset shows the initial stage of the cell voltage of (c).

and 1:2 (b′) electrolytes. This behaviour suggests that the aqueous electrolyte rapidly diffuses into the bottom of the PS layer through the dense surface layer and the anodization starts at the bottom of the PS layer, at notably smaller surfaces, resulting in an increase in real current density.

3.3. *Composition of porous silicon after anodization*

The transmission FTIR spectrum for a PS sample prepared in the 1:1 electrolyte is shown in Figure 3(a). The absorption peaks at 2114 cm^{-1} ($Si–H_2$, stretching) [37, 38], 2089 cm^{-1} (Si–H, stretching) [37, 38], 910 cm^{-1} ($Si–H_2$, scissoring) [1], and 667 cm^{-1} (Si–H) [1], disappeared upon anodization for 5 min in 0.02 M KNO_3–EG electrolyte and new absorption peaks appeared at 1068 cm^{-1} (siloxane, –Si–O–Si–, asymmetric stretching) [1, 38, 39], 455 cm^{-1} (Si–O) [40, 41], and 880 cm^{-1} (Si–OH) [40] (Figure 3(b)). However, no absorption peaks which are assignable to the products of reaction with the ethylene glycol appeared. This suggests that the PS surface coordinated with water present as an impurity in ethylene glycol and behaved in a manner similar to that in aqueous media (see Figure 3(e) and (f)). The broad absorption peaks around 1256 ~ 1070 cm^{-1} are characteristic of the oxidization products of PS samples (compare (b)–(f) with (g) in Figure 3) [10, 39]. Martinet and Devine [41] reported that SiO_2 showed vibrational absorption peaks at 1090 ~ 1060 cm^{-1} (TO mode) and 1256 cm^{-1} (LO mode), and the former shifted to lower values with thinning of –Si–O film (i.e., 1076 cm^{-1}: 120 nm, 1066 cm^{-1}: 2 nm). The broad absorption peaks imply the existence of various siloxane linkages of

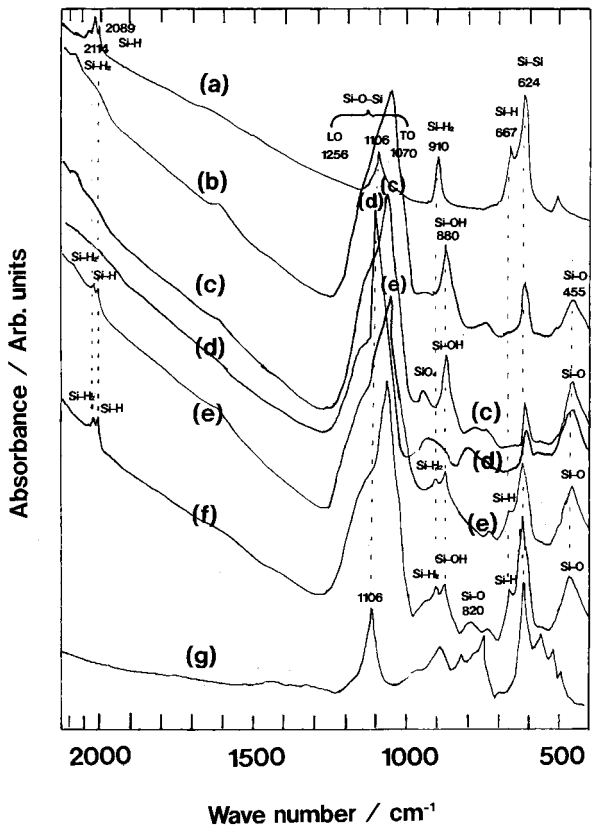

Fig. 3. Changes in transmission FTIR spectra of the PS sample prepared in 1:1 electrolyte and the flat Si sample, with anodization. (a) As-prepared PS sample; (b), (c) and (d) PS samples anodized in 0.02 M KNO_3–EG electrolyte for 5, 10 and 30 min, respectively; (e) the PS sample anodized in aqueous 0.02 M KNO_3 electrolyte for 5 min; (f) the PS sample anodized in HCl:H_2O (1:7) electrolyte for 10 min; and (g) flat Si sample anodized for 10 min in 0.02 M KNO_3–EG electrolyte.

various lengths depending on the size of the nano-ordered silicon particles (Figure 3(b)). With the prolonged anodization (i.e., 30 min), however, the Si–O absorption peaks reduced in intensity in the low wave number region of 1070 $\sim$ 1060 cm^{-1}. This shows that the nano-structured silicon layers were lost with anodization for a long period. The high resolution SEM supports this result. In addition to the above result, the absorption peaks at 880 cm^{-1} (Si–OH) [40] disappeared with prolonged anodization (Figure 3(d)). This implies that Si–OH is deprotonated completely (see Equation 4) in the electrolyte when the concentration of H^+ becomes very low since the anodization consumes H_2O impurity in the ethylene glycol.

For the PS sample prepared in 1:1 electrolyte and anodized in HCl:H_2O (1:7) electrolyte for 10 min, Si–H_2 (2114 cm^{-1}, 910 cm^{-1}) and Si–H absorption peaks (2089 cm^{-1}) remained in spite of intense Si–O absorption peaks (1106 cm^{-1}) (Figure 3(f)). The retention of Si–H_2 and Si–H proves that the anodization took place at the bottom of the porous layer. The HCl:H_2O (1:7) electrolyte easily diffuses into the grain boundaries of nano-ordered particles to reach the bottom of the porous layer because of its low viscosity (1.4×10^{-3} kg m^{-1} s^{-1} at 20 °C). Once the electrolyte has diffused, current is concentrated at the bottom of the PS layer to anodize it because of the low resistivity (2.3 Ω cm) of the electrolyte. In contrast, ethylene glycol is highly viscous (19.9×10^{-3} kg m^{-1} s^{-1} 20 °C) and has difficulties diffusing into the boundaries of nano-ordered particles. Furthermore, ethylene glycol has a high resistivity (9.3×10^{-3} Ω cm at 0.02 M KNO_3–EG), and the current flows at the top surface of the nano-ordered silicon layer.

To oxidize the surface of nano-ordered silicon particles by anodization, the use of an electrolyte with low H^+ concentration is recommended for easy removal of H^+ from silicon hydrate. Other requirements for the electrolyte are a high resistivity to concentrate the current on the nano-structured silicon surface and a high viscosity to prevent the diffusion of the electrolyte into the boundaries of the nano-ordered particles. Ethylene glycol fulfills these requirements.

3.4. *Morphological change of porous silicon with KNO_3–EG anodization*

The high-resolution SEM image showed that the as-prepared PS sample in 1:1 electrolyte was uniformly covered with a dense surface layer (Figure 4(a)-1). High resolution TEM confirmed that the dense surface layer considered of nano-ordered silicon particles. The enlarged cross section showed that the underlying layer (thickness: approximately 15 mm) was composed of two kinds of pillars with nano-ordered or nonnano-ordered areas. No spaces were observed between them (Figure 4(a)-3).

After anodization for 5 min in the KNO_3–EG electrolyte, however, the dense surface layer was cracked and the underlying layer formed porous structures with channels of approximately 1 $\sim$ 2 mm diameter (Figure 4(b)-1). The enlarged cross section showed that the anodization produced spaces between the nano- and nonnano-ordered areas of the underlying layer (Figure 4(b)-3). These were induced by peeling off of the nano-ordered silicon layers at the boundaries of nano- and nonnano-ordered areas, since the anodic current was concentrated at the most conductive sites among the areas in contact with the electrolyte. With the passage of the anodic current, –$(Si)_n$– bonds were split into –$(Si)_{n/m}$–O resulting in the formation of more fragile particles.

For the as-prepared PS sample in 1:2 electrolyte, the dense surface layer began to crack (Figure 5(a) top) and the underlying layer (thickness: approximately 14 μm) formed porous structures (Figure 5(a) bottom). After anodization for 5 min, the nano-ordered particles peeled off completely (Figure 5(b) top), and the nonnano-ordered silicon layers remained (Figure 5(b) bottom). It is considered that the disappearance of the PL is caused by the peeling off of the dense surface layer as mentioned above.

For the as-prepared PS sample in 1:4 electrolyte, most of the dense surface layer was peeled off and only the

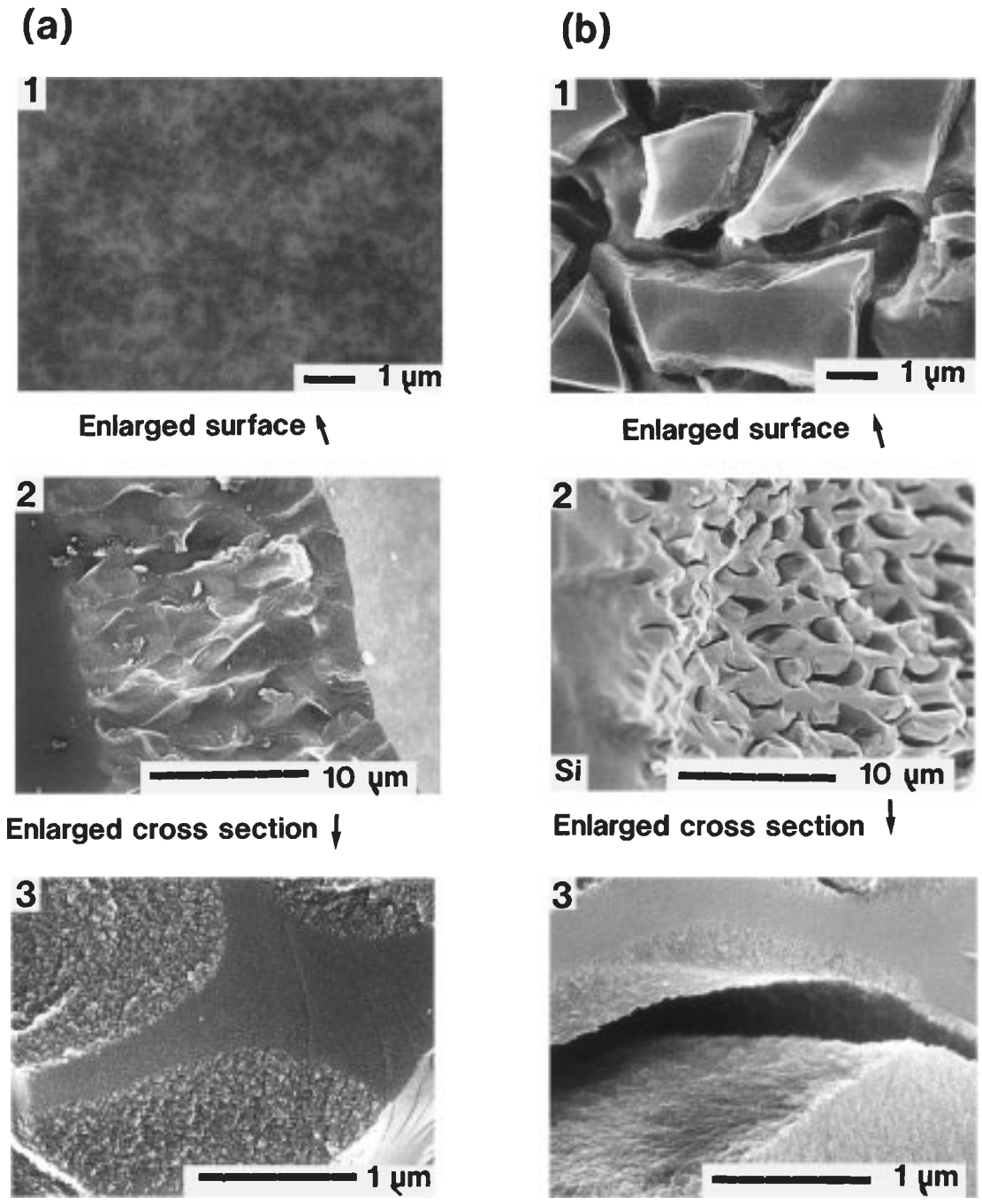

Fig. 4. SEM images of the as-prepared PS sample in 1:1 electrolyte. (a) As prepared, and (b) anodized in 0.02 M KNO_3–EG electrolyte for 5 min.

underlying layer was left (thickness: approximately 10 μm, pore diameter: approximately 2.5 $\sim$ 3.5 μm) (Figure 6(a) top) during the preparation. Anodization scarcely changed the morphology of the PS sample, suggesting that the anodization proceeded at the bottom of the porous layer containing the most conductive sites.

4. Conclusion

To electrochemically and effectively change Si–H of a nano-ordered silicon surface to Si–O and to stabilize the PL intensity, PS samples were anodized in 0.02 M KNO_3–EG electrolyte because ethylene glycol has high resistivity, high viscosity and good electrochemical stability. The PS sample prepared in 1:1 (49% HF:99.5% EtOH) electrolyte showed a 15-fold increase in the I_{max} of PL (excitation: 420 nm light) and a blue shift of I_{max} (>800 nm $\rightarrow$ 735 nm). The –Si–H_x bonds on the nano-ordered silicon layer were changed to –Si–OH and then to –Si–O by anodizing in 0.02 M KNO_3–EG electrolyte. Ethylene glycol proved to be the best solvent for the anodization of nano-ordered silicon particles prepared in 1:1 (49% HF:99.5% EtOH) electrolyte. Prolonged anodization (>10 min) induced a decrease in I_{max} of PL. SEM observation showed that

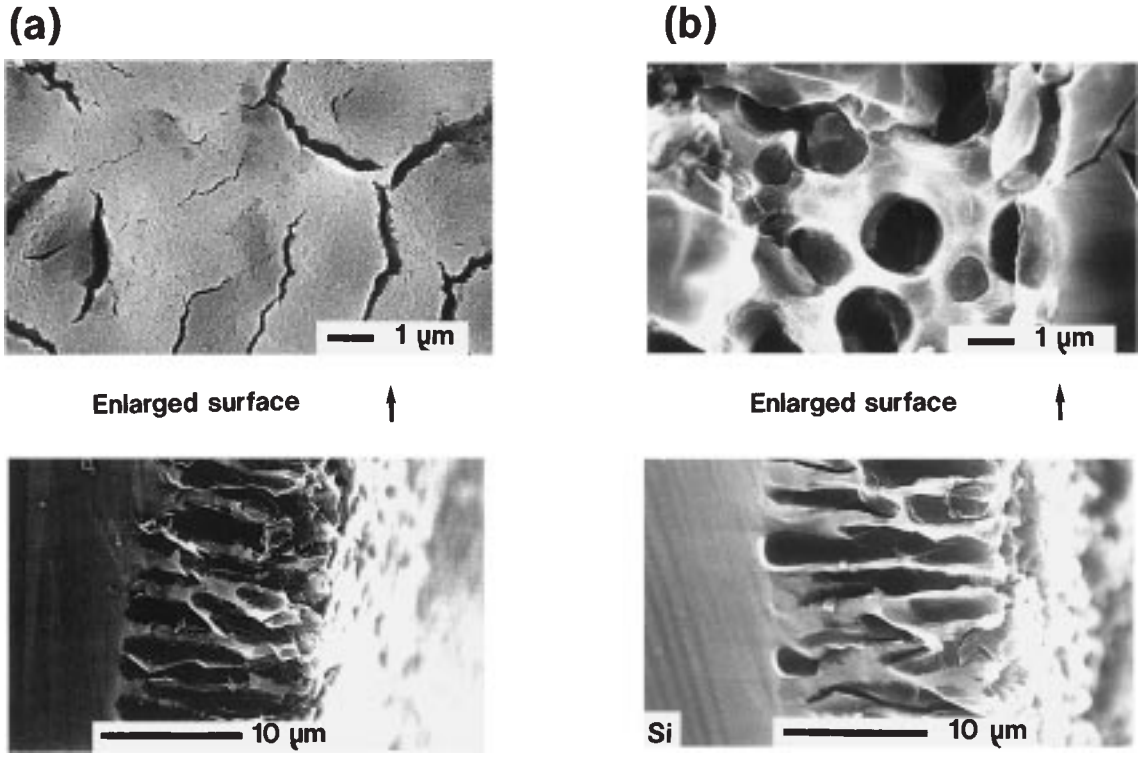

Fig. 5. SEM images of the PS samples prepared in 1:2 electrolyte. (a) As-prepared, and (b) anodized in the KNO_3–EG electrolyte for 5 min.

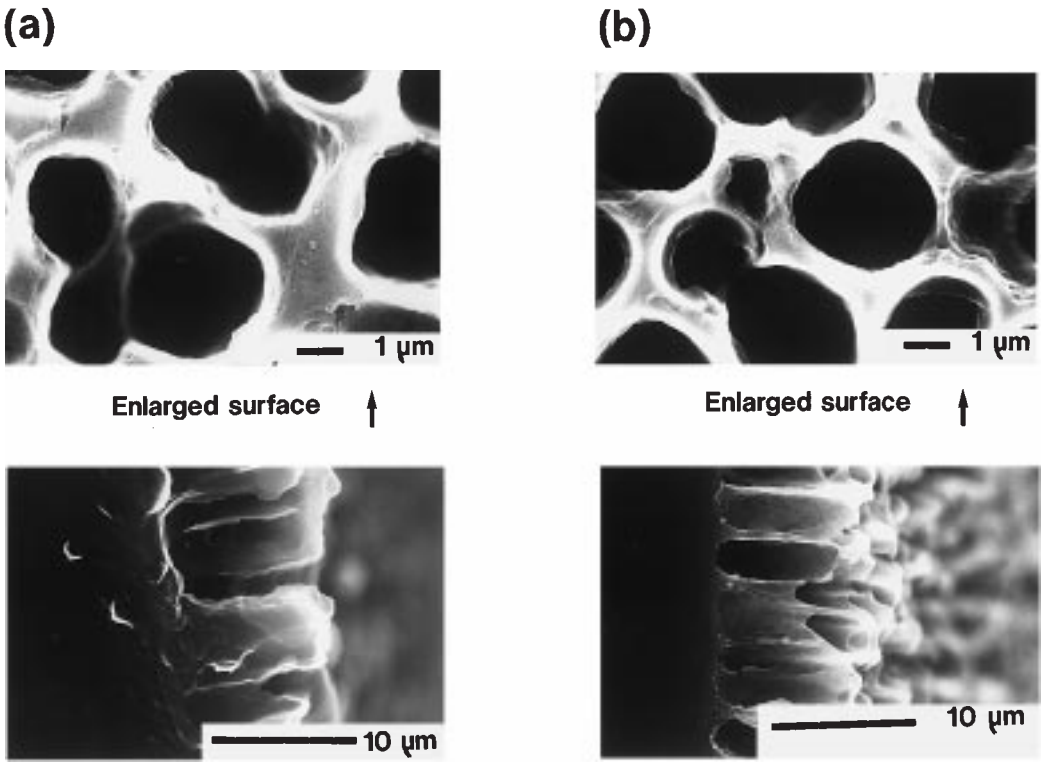

Fig. 6. SEM images of the PS samples prepared in 1:4 electrolyte. (a) As-prepared, and (b) anodized in 0.02 M KNO_3–EG electrolyte for 5 min.

the nano-ordered silicon particles did peel off. The small nano-particles tended to peel off, even in the preparation stage. The peeling off of the nano-ordered silicon particles led to a decrease in PL intensity.

Acknowledgement

This work was support by the Tokyo Ohka Foundation for the Promotion of Science and Technology.

References

1. C. Tsai, K-H. Li, J.C. Campbell, B.K. Hance and J.M. White, *J. Electron. Mater.* **21** (1992) 589.
2. M.A. Tischer, R.T. Collins, J.H. Stathis and J.C. Tsang, *Appl. Phys. Lett.* **60** (1992) 639.
3. N. Ookubo, H. Ono, Y. Ochiai, Y. Mochizuki and S. Matsui, *Appl. Phys. Lett.* **61** (1992) 940.
4. M. Shimasaki, Y. Show, M. Iwase, T. Izumi, T. Ichinohe, S. Nozaki and H. Morisaki, *Appl. Surf. Sci.* **92** (1996) 617.
5. S.M. Prokes, W.E. Carlos and V.M. Bermudes, *Appl. Phys. Lett.* **61** (1992) 1447.
6. T.J. McMahon and Y. Xiao, *Appl. Phys. Lett.* **63** (1993) 1657.
7. H. Yokomichi, H. Takakura, M. Kondo and K. Morigaki, *J. Non-Cryst. Solids,* **164–166** (1993) 957.
8. C. Delerue, G. Allan and M. Lannoo, *Phys. Rev. B* **48** (1993) 11024.
9. J. Salonen and E. Laine, *J. Appl. Phys.* **80** (1996) 5984.
10. C. Tsai, K.H. Li, J. Sarathy, S. Shih, J.C. Camplell, B.K. Hance and J.M. White, *Appl. Phys. Lett.* **59** (1991) 2814.
11. A.G. Cullis, L.T. Canham, G.M. Williams, P. W. Smith and O.D. Dosser, *J. Appl. Phys.* **75** (1994) 493.
12. S. Shih, C. Tsai, K.H. Li, H. Jung, J.C. Campbell and D.L. Kwong, *Appl. Phys. Lett.* **60** (1992) 633.
13. M. Yamada and K. Kondo, *Jpn. J. Appl. Phys.* **31** (1992) L993.
14. S.L. Zhang, K.S. Ho, Y. Hou, B. Qian, P. Diao and S. Cai, *Appl. Phys. Lett.* **62** (1993) 642.
15. A.J. Kontkiewicz, A.M. Kontkiewicz, J. Siejka, S. Sen, G. Nowak, A.M. Hoff, P. Sakthivel, K. Ahmed, P. Mukherjee, S. Witanach and J. Lagowski, *Appl. Phys. Lett.* **65** (1994) 1436.
16. S.L. Zhang, F.M. Huang, K.S. Ho, L. Jia, C.L. Yang, J.J. Li, T. Zhu, Y. Chen, S.M. Cai, A. Fujishima and Z.F. Liu, *Phys. Rev.* **51** (1995) 11194.
17. J.L. Batstone, M.A. Tischer and R.T. Collins, *Appl. Phys. Lett.* **62** (1993) 2667.
18. M. Shimura, M. Katsuma and T. Okumura, Abstracts of 1994 Autumn Meeting of the Electrochemical Society of Japan (1994) 91.
19. M. Katsuma, H. Ichikawa, T. Fujita, M. Shimura and T. Okumura, Abstracts II of the 55th Autumn Meeting, *Jpn. Soc. Appl. Phys.* (1994) 713.
20. M. Shimura, M. Katsuma and T. Okumura, *Jpn. J. Appl. Phys.* **35** (1996) 5730.
21. J.C. Vial, B.F. Gaspard, R. Herino, M. Ligeon, F. Muller, R. Romestain and R.M. Macfarlane, *Phys. Rev. B* **45** (1992) 14171.
22. T. Watanabe and S. Nakabayashi, Densiidou no Kagaku (Chemistry of Electron Transfer), Asakura-shoten, Tokyo (1996), p.116.
23. M. Pouraix, Atlas of Electrochem. Equilibria in Aqueous Solutions NACE, TX (1974) p. 459.
24. K. Funaki and Y. Shimizu, *Denki Kagaku* **28** (1960) 302, 358.
25. J.B. Peri, *J. Phys. Chem.* **69** (1965) 220.
26. M. Shimura, *J. Chem. Soc. Faraday Trans. 1* **72** (1976) 2248.
27. S. Tajima, Y. Tanabe, M. Shimura and T. Mori, *Electrochim. Acta* **6** (1962) 127.
28. M. Shimura and S. Tajima, *Denki Kagaku* **36** (1968) 377.
29. M. Shimura and S. Tajima, *Denki Kagaku* **40** (1972) 675.
30. A.J. van Roosmalen and J.C. Mol, *J. Phys. Chem.* **82** (1978) 2748.
31. J.B. Peri, *J. Phys. Chem.* **70** (1966) 2937.
32. H.P. Boehm, *Angew. Chem.* **78** (1966) 617.
33. J.L. Gole, F.P. Dudel, D. Grantier and D.A. Dixon, *Phys. Rev. B* **56** (1997) 2137.
34. Z. Sui, P.P. Leong and I.P. Herman, G.S. Highasi and H. Temkin, *Appl. Phys. Lett.* **60** (1992) 2086.
35. M. Shimura, M. Katsuma and T. Okumura, *ECS* 190th Meeting, **96-2**, (1996) 728.
36. M. Shimura, M. Katsuma, T. Chikuma and T. Okumura, 1997 *ECS and ISE Joint Meeting*, **97-2**, (1997) 1740.
37. Y. Ogata, H. Niki, T. Sakka and M. Iwasaki, *J. Electrochem. Soc.* **142** (1995) 1595.
38. T. Ban, T. Koizumi, S. Haba, N. Koshida and Y. Suda, *Jpn. J. Appl. Phys.* **33** (1994) 5603.
39. S. Shih, K.H. Jung, D.L. Kwong, M. Kovar and J.M. White, *Appl. Phys. Lett.* **62** (1993) 1780.
40. R.C. Anderson, R.S. Muller and C.W. Tobias, *J. Electrochem. Soc.* **140** (1993) 1393.
41. C. Martinet and R.A.B. Devine, *J. Appl. Phys.* **77** (1995) 4343.